Cardiac ECM Structure-Mimetic Electrospun Scaffolds Reinstate Healthy Cardiomyocyte Phenotype

By

Rutwik Rath

Thesis

Submitted to the Faculty of the

Graduate School of Vanderbilt University

in partial fulfillment of the requirements

for the degree of

MASTER OF SCIENCE

in

Biomedical Engineering

August, 2014

Nashville, Tennessee

Approved:

Hak-Joon Sung, Ph.D.

Douglas B. Sawyer, M.D., Ph.D.

ACKNOWLEDGEMENTS

Funding for this work was provided by NIH HL091465, NSF DMR 1006558, and AHA 13GRNT16690019. The authors would also like to acknowledge the use of resources at the Vanderbilt Institute of Nanoscale Science and Engineering (VINSE), a facility renovated under NSF ARI-R2 DMR-0963361. Confocal images were performed in part through the use of the VUMC Cell Imaging Shared Resource (supported by NIH grants CA68485, DK20593, DK58404, HD15052, DK59637 and EY08126). Printed poly (ε-caprolactone) (PCL) fiber scaffolds were provided by Dr. William Hofmesiter and Deepak Rajput from the University of Tennessee Space Institute. I would also like to thank my parents, Gitanjali Rath and Mihira Rath, and brother, Mrinal Rath, for their love and support.

TABLE OF CONTENTS

LIST OF FIGURES

LIST OF ABBREVIATIONS

Abbreviation	Full Name
1. MI	Myocardial infarction
2. ECM	Extracellular matrix
3. CM	Cardiomyocyte
4. TCPS	Tissue culture polystyrene
5. ELSP	Electrospinning
6. PCL	Poly (ε-caprolactone)
7. SEM	Scanning electron microscope
8. PCR	Polymerase chain reaction
9. IF	Immunofluorescnce

CHAPTER 1

INTRODUCTION

1.1 Motivation

Heart disease is the leading cause of death in the western world. Evidence in recent years has confirmed that pathophysiologic expressions of various cardiovascular diseases, including ischemic myocardial infarction (MI), is perpetuated by the myocardial extracellular matrix (ECM)(Gallagher, Jackson, & Hunyor, 2007). In a structurally normal heart, the number and location of cell-cell and cell-matrix connections prevent slippage of adjacent cardiomyocytes (CMs). In pathological states, the ECM becomes unregulated resulting in an increase in stiffness due to up-regulation of matrix deposition, and disorganization. This process of active remodeling, in response to MI by matrix metalloproteinases and cardiac fibroblast cells(Swynghedauw, 1999), results in a heterogeneous ECM composition and organization which in turn affects the overall geometry and function of the adult heart(Spinale, 2007).

1.2 Introduction

Cardiac Extracellular Matrix

The myocardial extracellular matrix (ECM) is a complex architectural network(Spinale, 2007) composed of glycoproteins, proteoglycans, and glycosaminoglycans(Rienks, Papageorgiou, Frangogiannis, & Heymans, 2014). The ECM acts as a dynamic microenvironment, with gradual changes in composition and organization over time(Kassiri & Khokha, 2005), to regulate key cardiac cell functions and control mechanisms(Jacot, McCulloch, & Omens, 2008). During development, the ECM plays a key role in spatiotemporal regulation of CM cell migration, reorganization, and differentiation(Lockhart, Wirrig, Phelps, & Wessels, 2011), resulting in highly organized CM orientation and myocardial fiber angle(D. D. Streeter, Jr., Spotnitz, Patel, Ross, & Sonnenblick, 1969). The resulting well-ordered and fiber-wound cells create a continuum of muscle fiber from the endocardium to the epicardium(D. D. Streeter & Bassett, 1966).

Then, complex and specific folding creates the secondary and tertiary structures of the adult heart(Corno, Kocica, & Torrent-Guasp, 2006).

Models for Native and Diseased Cardiomyocytes (CMs)

Presently, neonatal cardiomyocyte cultured on tissue culture polystyrene (TCPS)(Castaldo et al., 2013) have been used as cell source for heart disease research due to their versatility and convenience compared to other CMs(Sander, Suñe, Jopling, Morera, & Belmonte, 2013). Although other CM cell sources (including induced pluripotent stem cells and embryonic stem cells) have been previously investigated; a physiologically robust candidate for heart disease research, however, still remains to be found(Parameswaran, Kumar, Verma, & Sharma, 2013). Research with the neonatal CMs cultured on TCPS model has enabled morphological, biochemical and electrophysiological characterization of the heart(Louch, Sheehan, & Wolska, 2011) and has provided insight into changes resulting from MI(Chlopcikova, Psotova, & Miketova, 2001). The major limitations of such prior studies, however, is that when cultured *in vitro*, CMs readily undergo cellular remodeling of their actin/myosin structure, taking on a pleomorphic cell shape(Bugaisky & Zak, 1989). The change in cell morphology, which is directly influenced by the cell culture substrate surface, results in functional changes directly linked cell shape alterations(Mitcheson, Hancox, & Levi, 1998). These changes can even be seen at the gene level, with the re-expression of certain fetal genes such as smooth muscle α-actin(Morrisey, 2011). Cultured CMs are therefore phenotypically different from those present in the heart (*in vivo)*(Ausma & Borgers, 2002) ,resulting in a need for a culture system that better retains the *in vivo* CM phenotype for use in physiologically relevant cell studies conducted *in vitro*.

1.3 Contributions

The goal of this work is to address the need for a culture system that better retains the *in vivo* CM phenotype for use in physiologically relevant cell studies conducted *in vitro*. The experiments tested how key scaffold structural characteristics (fiber alignment, spacing, and diameter) regulate myocardial cell phenotype – specifically cell morphology, actin/myosin patterning, and cardiac gene expression. The

results helped establish a causal relationship between the ECM structure and maintenance of CM phenotype.

CHAPTER 2

METHODOLOGY

2.1 Aligned and Unaligned Poly (ε-caprolactone) Fiber Scaffold Fabrication

Fiber scaffolds were fabricated by an electrospinning (ELSP) technique. For the ELSP, a 12.5 wt. % poly (ε-caprolactone)(PCL, Sigma–Aldrich, 80 kDa) solution was prepared and dissolved in a 4:1 volume solution of chloroform(Sigma-Aldrich): methanol(Sigma-Aldrich) via continuous vortexing to dissolve pelletized PCL. The solution was placed in a 3 cc plastic syringe(Cadence Science) fitted with a 22 gauge blunt tip stainless steel needle(EFD Precision Tips) and electrospun using an electrospinner(NABOND Nano E-spinning System) set between 9-10 kV with a 10 cm tip-to-collector distance and a 0.2-0.5 mL/hr flow rate. PCL fibers were electrospun and deposited for 5 min on a custom made parallel plate setup with a spacing of 1.5 cm and then collected onto 15 mm rubber O-rings(McMaster-Carr). The fibers collected O-rings, which were placed in a vacuum overnight to ensure removal of residual solvents. The dried fibers were then placed in between custom-made 1mm thick PDMS O-rings with an outer diameter of 12 mm and an inner diameter of 8 mm(Miltex® Biopsy Punch) to maintain the organized structure of the fibers, while preserving the elasticity of the PCL.

2.2 Scaffold Analysis

Scaffold constructs were dehydrated in a graded series of ethanol in deionized water (50%, 70%, 85%, 90%, and then 100% ethanol) followed by ethanol removal via vacuum overnight to remove any water in preparation for scanning electromicroscopy. The dehydrated samples were then sputter coated with an ATC 2200(AJA International, Inc.) gold sputter coater for 60 seconds and imaged using a Scanning Electron Microscope(SEM, Hitachi S4200) in the ViNSE Institute at Vanderbilt University.

2.3 Cardiomyocyte Isolation

All animal procedures were conducted according to the guidelines of the Vanderbilt University Animal Care and Use Committee. Ventricular CMs from 2 day old and 7 week old rat hearts were isolated and cultured using previously described protocols(Ehler, Moore-Morris, & Lange, 2013; Eppenberger-Eberhardt et al., 1991).

2.4 Scaffold Seeding and Cell Culture

PCL fiber scaffolds were sterilized for 1 hr under UV, coated for 2 hrs with 250 µL of 10 mg/mL whole mouse laminin(Fisher) at room temperature. Cells were then seeded at 60,000 cells/cm^2 and allowed to adhere for 3 hrs in DMEM(Sigma) + 7% bovine serum(Sigma) containing 0.1mM BrdU(Sigma, to prevent division and over growth of non-CM cells) and 25 µM blebbistatin to prevent contraction. Cells were then switched to defined serum free media for phenotypic studies(Ellingsen et al., 1993) and cultured overnight (12-15 hrs) with 25 µM blebbistatin. The next day, cells were incubated for 1 hr in serum free media + 20 mM KCl(Sigma) (without blebbistatin) to allow for the reforming of sarcomere structures in diastole. Cells were then fixed and treated for the appropriate endpoint assays.

2.5 Cardiomyocyte Morphology Analysis

Scaffolds were rinsed several times with PBS, fixed in 4% paraformaldehyde solution, then rinsed again several times in PBS, and lastly imaged. The cells were then imaged on Nikon Eclipse Ti inverted fluorescence microscope using a Nikon DS-QiMc black and white camera for cell morphology analysis(Han et al., 2012). The images were acquired with Nikon Elements Advanced Research image analyzing computer software and imported into ImageJ(NIH, Bethesda, MA) for analysis. Average fiber angle, fiber thickness and porosity was determined using previously described methods in the ImageJ program(N. Wang et al., 2013).

2.6 Immunofluorescence Staining

On day 1 after the experiment, fixed scaffolds were permeabilized overnight in 0.2% Triton X-100 in PBS at 4 °C. On day 2, the Triton X-100 solution was removed and the cells were blocked in PBS containing 20% goat serum and 0.2% Triton X-100 in PBS overnight at 4°C. On day 3, after blocking, the scaffolds were incubated with a 1:200 primary mouse anti-myomesin antibody(C-16, SCBT) diluted in PBS containing 0.1% BSA and 0.2% Triton X-100 in PBS overnight at 4°C on a shaker at low speed. On day 4, the primary antibody solution was removed, the scaffolds were rinsed several times in PBS, and incubated with a 1:200 secondary goat anti-mouse Alexa 594-conjugated antibody(Abcam) diluted in PBS containing 0.1% BSA and 0.2% Triton X-100 in PBS overnight at 4°C in the dark on a shaker at low speed. On day 5, after 18 hours, the secondary antibody solution was removed; the scaffolds were rinsed several times in PBS, and stained with 200 μL 0.0016 μM Hoechst dye for 10 minutes at room temperature. The Hoechst stain was then removed and the scaffolds were rinsed several times in PBS, and then incubated with 200 μL of 0.16 μM AlexaFluor488-conjugated phalloidin(Life Tech, Carlsbad, CA) for 20 minutes at room temperature. The phalloidin was then removed and the cells were washed once in PBS for 10 minutes and 200 μL of PBS was added to the cells for use when imaging. Cells were imaged on the Nikon Eclipse Ti inverted fluorescence microscopes with a Nikon Digital Sight DS-Fi1 color camera using Nikon Elements Advanced Research image analyzing computer software. The images were imported into ImageJ(NIH, Bethesda, MA) to determine the average bandwidth of the actin and myosin fibers.

2.7 Polymerase Chain Reaction

For polymerase chain reaction (PCR), 10 ng cDNA prepared by Trizol(Life-Tech) isolation and cDNA Synthesis(Life-Tech) using the manufacture's recommended protocol, was mixed with PCR Master Mix(Life Tech) and 500 nM mRNA-specific primers for the specified genes (**F:**AGGAGGCACTGATTTGGCAG **R:**GGGAGGTCTGTAGGGAGTCCA, *α-MYH6;* **F:**CGAGAGATGGCTGCATTTGG **R:**TGGACTGGTTCTCCCGATCT, *β-MYH7;* **F:**GTGGATCGAGACCATGTGGG **R:**GCCGTCTGCCTGAGATGTA, *SCN5A.1*;

F:CTGTGCTACGTTCCTTCCGT **R:**ACTGTCCTCAGGGGTCTGTT, *SCN5A.2*;

F:CAGTCGCCATCAGGAACCTC **R:**CTGTCAGCAATGCCTGGGTA, α-*SMA*;

F:GAGTTGTATGGCACTTGGCG **R:**TGCGTAAGGGTTCAGCTTCA, *RPL4*).

Samples were then amplified in a PCR machine(Bio-Rad, model S1000)) with the following steps: 3 minutes at 95 °C to denature DNA, followed by 35 steps of 95 °C for 30 seconds (denaturation), 58 °C for 30 seconds (annealing), and 72 °C for 30 seconds (extension). Genes of interest included myosin heavy chain 6 and 7, sodium-voltage gated channel 5 isoform 1 and 2, and α-smooth muscle actin. Expression was normalized to 60 s ribosomal protein L4(RPL4).

2.8 Printed Poly (ε-caprolactone) (PCL) Fixed Fiber Spacing

Several different scaffolds made of PCL fibers were printed onto PVC backing, patterning a 1 cm^2 area with a pitch of 2 μm and spacing of either 2, 10, or 15 μm using previously described methods(Rajput et al., 2013). Scaffolds were sterilized for 1 hr under UV, coated for 2 hrs with 250 μL of 10 mg/mL whole mouse laminin(Fisher) at room temperature. Cells were then seeded at 60,000 cells/cm^2 and allowed to adhere for 3 hrs in DMEM(Sigma) + 7% bovine serum(Sigma) containing 0.1 mM BrdU(Sigma) and 25 μM blebbistatin to prevent contraction. Cells were then switched to defined serum free media for phenotypic studies(Ellingsen et al., 1993) and cultured overnight (12-15 hrs) with 25 μM blebbistatin. The next day, cells were then incubated for 1 hr in serum free media + 20 mM KCl(Sigma) (without blebbistatin) to allow for the reforming of sarcomere structures in diastole. Cells were then fixed and stained for actin and myosin (as previously described).

2.9 Statistical Analysis

Data are displayed as mean ± standard error mean. Average and standard deviations were calculated in Excel(Microsoft, Redmond, WA) and imported into GraphPad(GraphPad Software, La Jolla, CA) for statistical analysis. Data was statistically analyzed using one-way ANOVA and, if significance was found, further tested using a bonferroni post hoc test. A difference with $p<0.05$ was considered significant.

CHAPTER 3

RESULTS AND DISCUSSIONS

3.1 Creation of Poly (ε-caprolactone) Fiber Scaffolds

To determine if cardiac tissue-mimetic scaffolds can be made to mimic native decellularized donor (Figure 1a) and ischemic (Figure 1b) cardiac tissue, electrospun fibers made of poly(ε-caprolactone) (PCL) were fabricated and compared to representative acellular porcine tissue alignment (Figure 1c), fiber spacing (Figure 1d), and fiber diameter (Figure 1e). Porcine tissue and aligned PCL fiber scaffolds were not significantly different in alignment, spacing, or fiber diameter nor were the ischemic tissue/unaligned ECM.

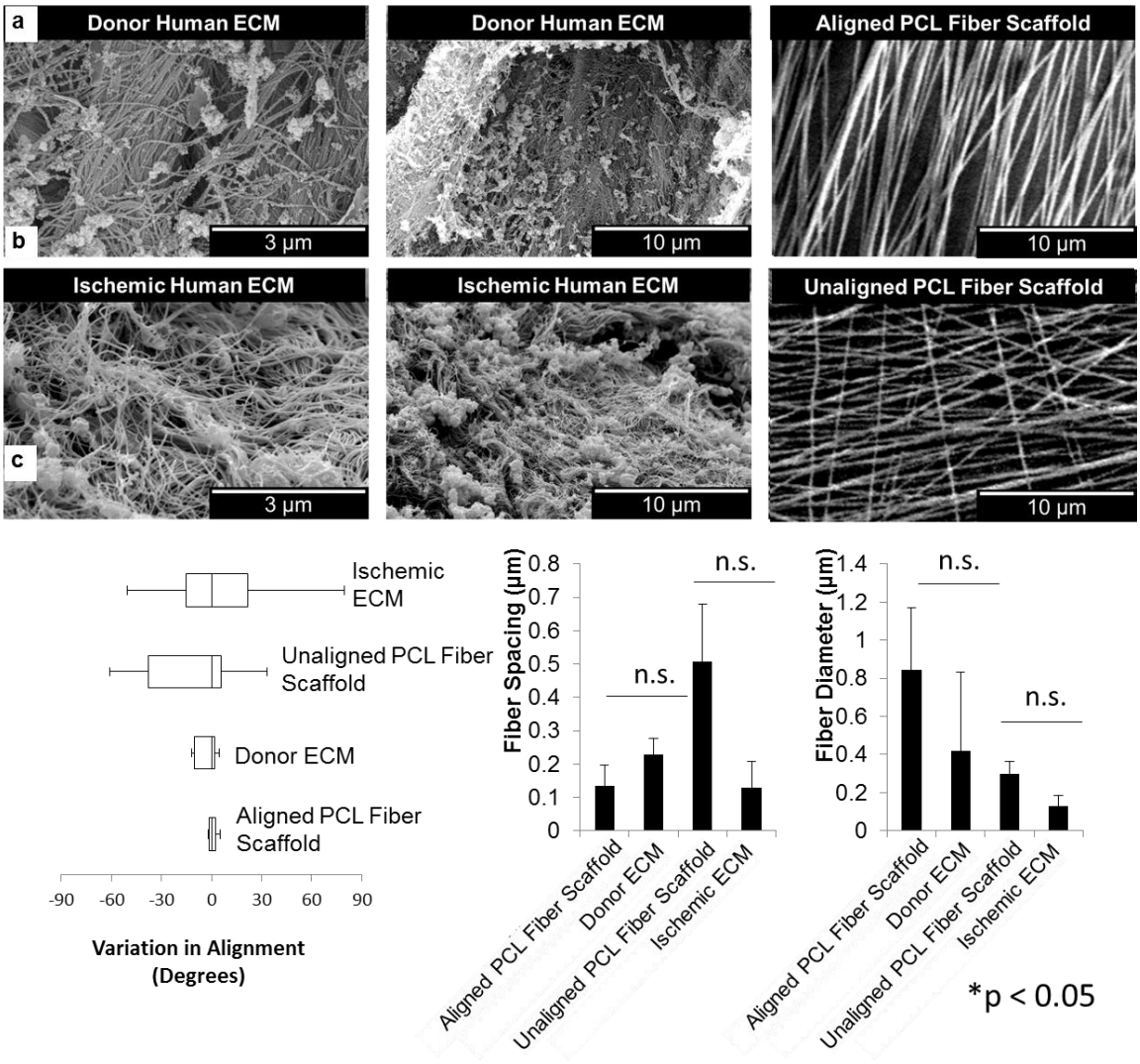

Figure 1 Characterization of decellularized human cardiac ECM and PCL fiber scaffold. (a) Representative scanning electron microscopy (SEM) images of donor human cardiac ECM and aligned PCL fiber scaffolds. (b) Representative SEM images of ischemic human cardiac ECM and unaligned PCL fiber scaffolds. Analysis of scaffold alignment (c), spacing between fibers (d), and fiber diameter (e) indicate no significant differences between the electrospun scaffolds and their correlative ECM matrices. *p<0.05

3.2 Actin/Myosin Staining and Morphological Analysis of Adult and Neonatal Cardiomyocytes

To determine the influence of scaffold organization on phenotype changes of adult and neonatal CMS, CMs were cultured on artificial PCL fiber scaffolds as well as TCPS and IF stained for actin and myosin (Figure 2a) and analyzed for cell morphology (Figure 2b). In adult CMs, IF staining showed patterning of equidistant actin and myosin bands for all test groups except cells cultured on unaligned PCL fiber scaffolds. Neonatal CMs cultured on unaligned PCL fiber scaffolds had unorganized/speckled actin and myosin bands for all groups except for cells cultured on aligned PCL fiber scaffolds, which showed banding patterns similar to adult CMs. Analysis of cell morphology indicated that adult cells cultured on aligned PCL fiber scaffolds had significantly higher aspect ratios versus unaligned PCL fiber scaffolds and spin-coated PCL, including no significant difference from TCPS cultured or freshly isolated adult CMs. Neonatal cells followed a similar trend with cells cultured on aligned PCL fiber scaffolds having significantly higher aspect ratios versus all other groups.

In culture, CMs remain rod-shaped and cross-striated for 24-48 hours, then that cell ends became progressively more rounded and start losing the striation pattern(Bugaisky & Zak, 1989). In our studies, we determined that on an aligned ECM matrix maintained the cell striation pattern and limited rounding. However, on a matrix of same composition but unaligned organization, the rounding and loss of striation patterning was accelerated. Such results support the idea that ECM structure controls cell morphology by promoting or preventing ultrastructural cell re-organization(Gerdes & Capasso, 1995).

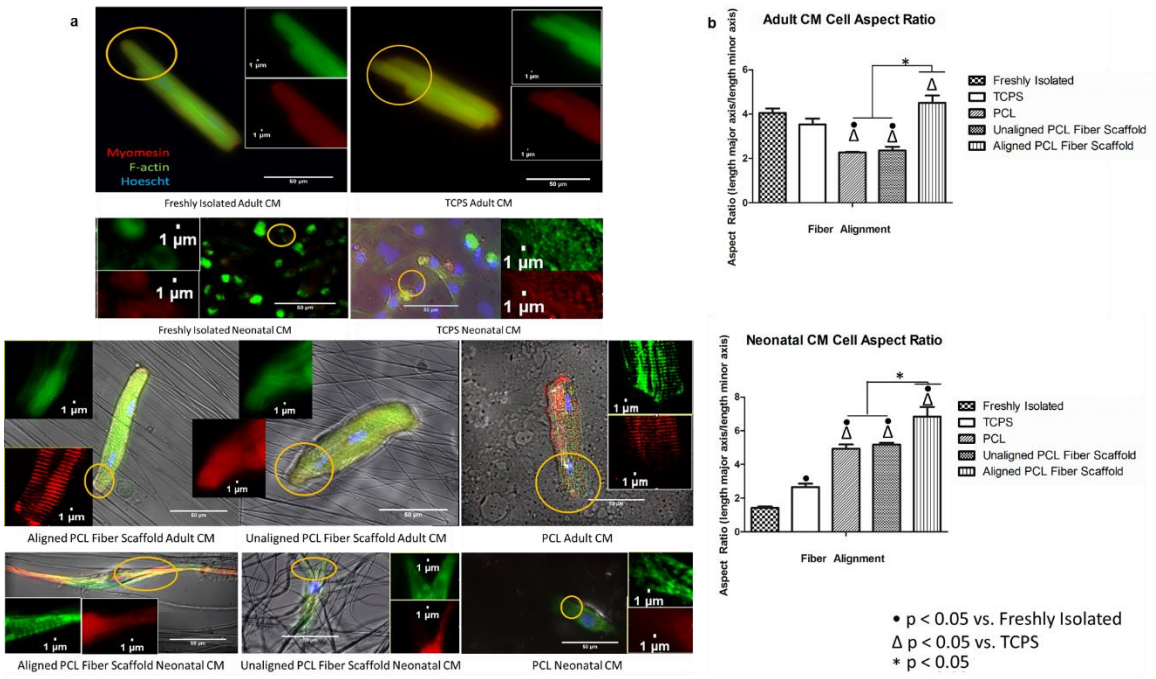

Figure 2 Actin/myosin staining and morphology analysis of adult and neonatal CMs. (a) Actin/myosin band staining of top (L,R) freshly isolated, tissue culture polystyrene (TCPS), and bottom (L,R) aligned PCL fiber scaffold, unaligned PCL fiber scaffold, and spin-coated polymer control (PCL) of adult (top) and neonatal (bottom) CMs. (b) Analysis of cell aspect ratio shows that adult CMs cultured on aligned PCL fiber scaffolds had greater aspect ratios versus all the test groups except for CMs on TCPS and freshly isolated CMs; neonatal CMs on aligned PCL fiber scaffolds has the greatest aspect ratio versus all the other neonatal CMs groups.*p<0.05

3.3 Cardiac Gene Expression

After IF staining, we focused on cardiac gene expression and, using adult CMs, we investigated the gene-level expression of key cardiac and de-differentiation genes to determine CM maintenance ability on its phenotype. The data shows representative cell SEM images (A) and PCR of cardiac differentiation markers (B) of freshly isolated CMs, aligned PCL fiber scaffolds, unaligned PCL fiber scaffolds, and TCPS. Analysis of the genes indicates activation of mature *β-MYH7*, and voltage gated sodium ion channels (without activation of dedifferentiation gene α-smooth muscle actin) in the freshly isolated CMs and CMs cultured on scaffolds but not in CMs cultured on TCPS. Only freshly isolated CMs showed activation of *α-MYH6*.

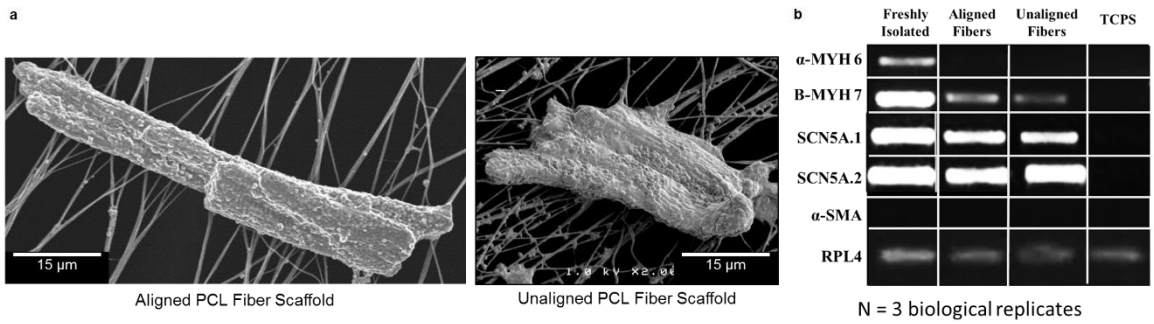

Figure 3 SEM imaging and PCR analysis of adult CMs. (a) Representative SEM images of CMs on aligned (L) and unaligned (R) PCL fiber scaffolds. (b) PCR analysis of adult CMs indicates continued expression of *β-MYH7* and *SCN5A1* and *SCN5A2* (without activation of α-smooth muscle actin) in CMs cultured on electrospun fibers, with complete suppression of all genes in CMs on TCPS.(*α-MYH6* – Alpha Myosin Heavy Chain 6; *β-MYH7* – Beta Myosin Heavy Chain 7; *SCN5A 1* – Sodium Channel, voltage-gated type 5 isoform 1; *SCN5A 2* – Sodium Channel, voltage-gated type 5 isoform 2; *α-SMA* – Alpha Smooth Muscle Actin; *RPL4* – 60S ribosomal protein L4 (housekeeping).

3.4 Poly (ε-caprolactone) Printed Fiber Scaffold Spacing and Cardiomyocyte Organization

In our studies, we determined that the spacing of fibers affects CM organization. On 2 μm spaced PCL fibers, CMs aligned perpendicular to the fibers, lying across the printed PCL fibers. At 5 μm spaced PCL fibers, CMs aligned 45° to the fibers. At 15 μm, slightly smaller than the average 20 μm width of the CMs, the CMslls sat in between the fibers, lying parallel to the fibers. Such results support the idea that ECM spacing controls cell morphology by promoting or preventing cell alignment relative to the fibers(S. Wang, Leon, & Roberge, 1996). Similar to previous findings, when NHCs were cultured on similarly patterned TCPS substrate, the CMs grew along a common axis in parallel with the lattice and expressed an *in vivo*-like phenotype(Simpson et al., 1994).

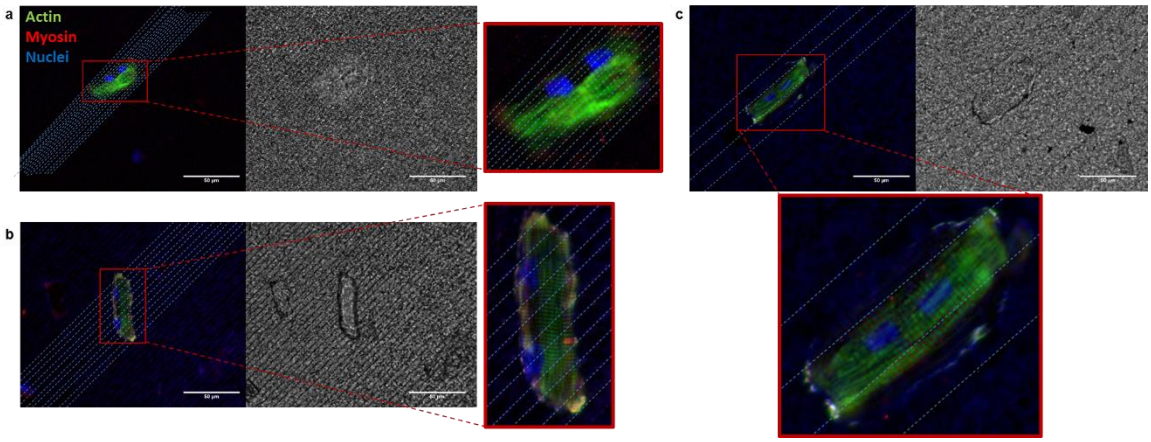

Figure 4 Actin/myosin staining of adult CMs on 2, 5, and 15 µm printed PCL fiber scaffolds. (a) Adult CMs on 2µm spaced printed PCL fibers. (b) Adult CM on 5µm spaced printed PCL fibers. (c) Adult CM on 15µm spaced printed PCL fibers. Blown out images are 1.35x the indicated boxed area. At 2 µm spacing, CMs aligned perpendicular to the fibers; at 5 µm spacing, CMs aligned 45° to the fibers; at 15 µm spacing, CMs aligned parallel to the fibers.

CHAPTER 4

CONCLUSIONS

Culturing CMs on TCPS for cell studies allows for the direct manipulation of cells, with control over of environmental parameters without external interference from compensatory feedback mechanisms(Bursac et al., 1999). Cultured cells, however, adapt to the culture environment by undergoing morphological transformations, often taking on a pleomorphic shape(Banyasz et al., 2008). The pleomorphic cells, whose morphology is influenced by the cell culture substrate surface, results in functional changes directly linked cell shape alterations(Mitcheson et al., 1998). Therefore, TCPS cultured cells cannot be considered to be in a functionally stable, steady-state representative of *in vivo* conditions(Akhyari, Kamiya, Haverich, Karck, & Lichtenberg, 2008). Therefore, cultured cells should be considered as a *complement* (rather than *replacement*) cell model for acutely isolated CMs, which is not possible with extended cell culture studies. Caution is needed when analyzing data from TCPS cultured cells as modifications of physiological properties (with time) could simply be a result of subtle changes to the culture conditions(Libby & Lee, 2000). To overcome these substrate limitations, previous research has investigated the use of decellularized ECM. Natural ECM is considered an ideal scaffold as it contains all the necessary components of the derived tissue(Sreejit & Verma, 2013). The decellularization process, however, disrupts the organization and architecture of the cells, changing the interplay among different ECM molecules(Crapo, Gilbert, & Badylak, 2011). In spite of the efforts to maintain the ECM, current methods of ECM decellularization suffer from damage to the structure of the matrix and contamination by decellularization agent residues.

Synthetic scaffolds have therefore been proposed as alternatives to decellularized ECM. Synthetic scaffolds offer more precise control over material properties and are: inexpensive, biocompatible,

easy to fabricate and have little to no batch-to-batch variation(Patel, Fine, Sandig, & Mequanint, 2006). Synthetic scaffolds do have a major disadvantage; there are currently no synthetic, feeder cell (or a cell that synthesizes ECM)-free approaches that enable the recapitulation of complex microenvironments *in vitro* both in terms of protein composition and spatial organization(Lutolf & Hubbell, 2005).

The results of this research indicate that the use of aligned PCL fiber scaffolds to maintian cardiac cell phenotype for extended periods of time, match freshly isolated cells both morpologically and genetically. The outcomes of this research have the potential to alter the field of tissue engineering by providing a tunable model that mimics the complex cardiac microenvironment *in vitro*, providing better models further understanding of the cardiomyocyte biology.

REFERENCES

Akhyari, P., Kamiya, H., Haverich, A., Karck, M., & Lichtenberg, A. (2008). Myocardial tissue engineering: the extracellular matrix. *European Journal of Cardio-Thoracic Surgery, 34*(2), 229-241. doi: 10.1016/j.ejcts.2008.03.062

Ausma, J., & Borgers, M. (2002). Dedifferentiation of atrial cardiomyocytes: from in vivo to in vitro. *Cardiovascular Research, 55*(1), 9-12. doi: 10.1016/s0008-6363(02)00434-0

Banyasz, T., Lozinskiy, I., Payne, C. E., Edelmann, S., Norton, B., Chen, B., . . . Balke, C. W. (2008). Transformation of adult rat cardiac myocytes in primary culture. *Experimental Physiology, 93*(3), 370-382. doi: 10.1113/expphysiol.2007.040659

Bugaisky, L. B., & Zak, R. (1989). Differentiation of adult rat cardiac myocytes in cell culture. *Circulation Research, 64*(3), 493-500. doi: 10.1161/01.res.64.3.493

Bursac, N., Papadaki, M., Cohen, R. J., Schoen, F. J., Eisenberg, S. R., Carrier, R., . . . Freed, L. E. (1999). *Cardiac muscle tissue engineering: toward an in vitro model for electrophysiological studies* (Vol. 277).

Castaldo, C., Di Meglio, F., Miraglia, R., Sacco, A. M., Romano, V., Bancone, C., . . . Nurzynska, D. (2013). Cardiac fibroblast-derived extracellular matrix (biomatrix) as a model for the studies of cardiac primitive cell biological properties in normal and pathological adult human heart. *Biomed Res Int, 2013*, 352370. doi: 10.1155/2013/352370

Chlopcikova, S., Psotova, J., & Miketova, P. (2001). Neonatal rat cardiomyocytes--a model for the study of morphological, biochemical and electrophysiological characteristics of the heart. *Biomedical papers of the Medical Faculty of the University Palacký, Olomouc, Czechoslovakia, 145*(2), 49-55.

Corno, A. F., Kocica, M. J., & Torrent-Guasp, F. (2006). The helical ventricular myocardial band of Torrent-Guasp: potential implications in congenital heart defects. *Eur J Cardiothorac Surg, 29 Suppl 1*, S61-68. doi: 10.1016/j.ejcts.2006.02.049

Crapo, P. M., Gilbert, T. W., & Badylak, S. F. (2011). An overview of tissue and whole organ decellularization processes. *Biomaterials, 32*(12), 3233-3243. doi: http://dx.doi.org/10.1016/j.biomaterials.2011.01.057

Ehler, E., Moore-Morris, T., & Lange, S. (2013). Isolation and Culture of Neonatal Mouse Cardiomyocytes. *Journal of Visualized Experiments*(79), e50154. doi: doi:10.3791/50154

Ellingsen, O., Davidoff, A. J., Prasad, S. K., Berger, H. J., Springhorn, J. P., Marsh, J. D., . . . Smith, T. W. (1993). Adult rat ventricular myocytes cultured in defined medium: phenotype and electromechanical function. *American Journal of Physiology, 265*(2 Pt 2), H747-754.

Eppenberger-Eberhardt, M., Riesinger, I., Messerli, M., Schwarb, P., Muller, M., Eppenberger, H. M., & Wallimann, T. (1991). Adult rat cardiomyocytes cultured in creatine-deficient medium display large mitochondria with paracrystalline inclusions, enriched for creatine kinase. *Journal of Cell Biology, 113*(2), 289-302.

Gallagher, G. L., Jackson, C. J., & Hunyor, S. N. (2007). Myocardial extracellular matrix remodeling in ischemic heart failure. *Front Biosci, 12*, 1410-1419.

Gerdes, A. M., & Capasso, J. M. (1995). Structural remodeling and mechanical dysfunction of cardiac myocytes in heart failure. *J Mol Cell Cardiol, 27*(3), 849-856.

Han, N., Johnson, J. K., Bradley, P. A., Parikh, K. S., Lannutti, J. J., & Winter, J. O. (2012). Cell attachment to hydrogel-electrospun fiber mat composite materials. *Journal of Functional Biomaterials, 3*(3), 497-513. doi: 10.3390/jfb3030497

Jacot, J. G., McCulloch, A. D., & Omens, J. H. (2008). Substrate stiffness affects the functional maturation of neonatal rat ventricular myocytes. *Biophys J, 95*(7), 3479-3487. doi: 10.1529/biophysj.107.124545

Kassiri, Z., & Khokha, R. (2005). Myocardial extra-cellular matrix and its regulation by metalloproteinases and their inhibitors. *Thromb Haemost, 93*(2), 212-219. doi: 10.1267/thro05020212

Libby, P., & Lee, R. T. (2000). Matrix matters. *Circulation, 102*(16), 1874-1876.

Lockhart, M., Wirrig, E., Phelps, A., & Wessels, A. (2011). Extracellular matrix and heart development. *Birth Defects Res A Clin Mol Teratol, 91*(6), 535-550. doi: 10.1002/bdra.20810

Louch, W. E., Sheehan, K. A., & Wolska, B. M. (2011). Methods in cardiomyocyte isolation, culture, and gene transfer. *Journal of Molecular and Cellular Cardiology, 51*(3), 288-298. doi: 10.1016/j.yjmcc.2011.06.012

Lutolf, M. P., & Hubbell, J. A. (2005). Synthetic biomaterials as instructive extracellular microenvironments for morphogenesis in tissue engineering. *Nat Biotech, 23*(1), 47-55.

Mitcheson, J. S., Hancox, J. C., & Levi, A. J. (1998). Cultured adult cardiac myocytes: Future applications, culture methods, morphological and electrophysiological properties. *Cardiovascular Research, 39*(2), 280-300. doi: 10.1016/s0008-6363(98)00128-x

Morrisey, Edward E. (2011). Rewind to Recover: Dedifferentiation after Cardiac Injury. *Cell Stem Cell, 9*(5), 387-388.

Parameswaran, S., Kumar, S., Verma, R. S., & Sharma, R. K. (2013). Cardiomyocyte culture — an update on the in vitro cardiovascular model and future challenges. *Canadian Journal of Physiology and Pharmacology, 91*(12), 985-998. doi: 10.1139/cjpp-2013-0161

Patel, A., Fine, B., Sandig, M., & Mequanint, K. (2006). Elastin biosynthesis: The missing link in tissue-engineered blood vessels. *Cardiovasc Res, 71*(1), 40-49. doi: 10.1016/j.cardiores.2006.02.021

Rajput, D., Crowder, S. W., Hofmeister, L., Costa, L., Sung, H. J., & Hofmeister, W. (2013). Cell interaction study method using novel 3D silica nanoneedle gradient arrays. *Colloids Surf B Biointerfaces, 102*, 111-116. doi: 10.1016/j.colsurfb.2012.07.044

Rienks, M., Papageorgiou, A.-P., Frangogiannis, N. G., & Heymans, S. (2014). Myocardial Extracellular Matrix: An Ever-Changing and Diverse Entity. *Circulation Research, 114*(5), 872-888. doi: 10.1161/circresaha.114.302533

Sander, V., Suñe, G., Jopling, C., Morera, C., & Belmonte, J. C. I. (2013). Isolation and in vitro culture of primary cardiomyocytes from adult zebrafish hearts. *Nature Protocols, 8*(4), 800-809. doi: http://www.nature.com/nprot/journal/v8/n4/abs/nprot.2013.041.html#supplementary-information

Simpson, D. G., Terracio, L., Terracio, M., Price, R. L., Turner, D. C., & Borg, T. K. (1994). Modulation of cardiac myocyte phenotype in vitro by the composition and orientation of the extracellular matrix. *Journal of Cellular Physiology, 161*(1), 89-105. doi: 10.1002/jcp.1041610112

Spinale, F. G. (2007). *Myocardial Matrix Remodeling and the Matrix Metalloproteinases: Influence on Cardiac Form and Function* (Vol. 87).

Sreejit, P., & Verma, R. S. (2013). Natural ECM as biomaterial for scaffold based cardiac regeneration using adult bone marrow derived stem cells. *Stem Cell Rev, 9*(2), 158-171. doi: 10.1007/s12015-013-9427-6

Streeter, D. D., & Bassett, D. L. (1966). An engineering analysis of myocardial fiber orientation in pig's left ventricle in systole. *The Anatomical Record, 155*(4), 503-511. doi: 10.1002/ar.1091550403

Streeter, D. D., Jr., Spotnitz, H. M., Patel, D. P., Ross, J., Jr., & Sonnenblick, E. H. (1969). Fiber orientation in the canine left ventricle during diastole and systole. *Circ Res, 24*(3), 339-347.

Swynghedauw, B. (1999). *Molecular Mechanisms of Myocardial Remodeling* (Vol. 79).

Wang, N., Burugapalli, K., Song, W., Halls, J., Moussy, F., Zheng, Y., . . . Li, K. (2013). Tailored fibro-porous structure of electrospun polyurethane membranes, their size-dependent properties and trans-membrane glucose diffusion. *Journal of Membrane Science, 427*(0), 207-217. doi: http://dx.doi.org/10.1016/j.memsci.2012.09.052

Wang, S., Leon, L. J., & Roberge, F. A. (1996). Interactions between adjacent fibers in a cardiac muscle bundle. *Ann Biomed Eng, 24*(6), 662-674.